iScience

CellPress
OPEN ACCESS

Article

# A novel *in vivo* system to study coral biomineralization in the starlet sea anemone, *Nematostella vectensis*

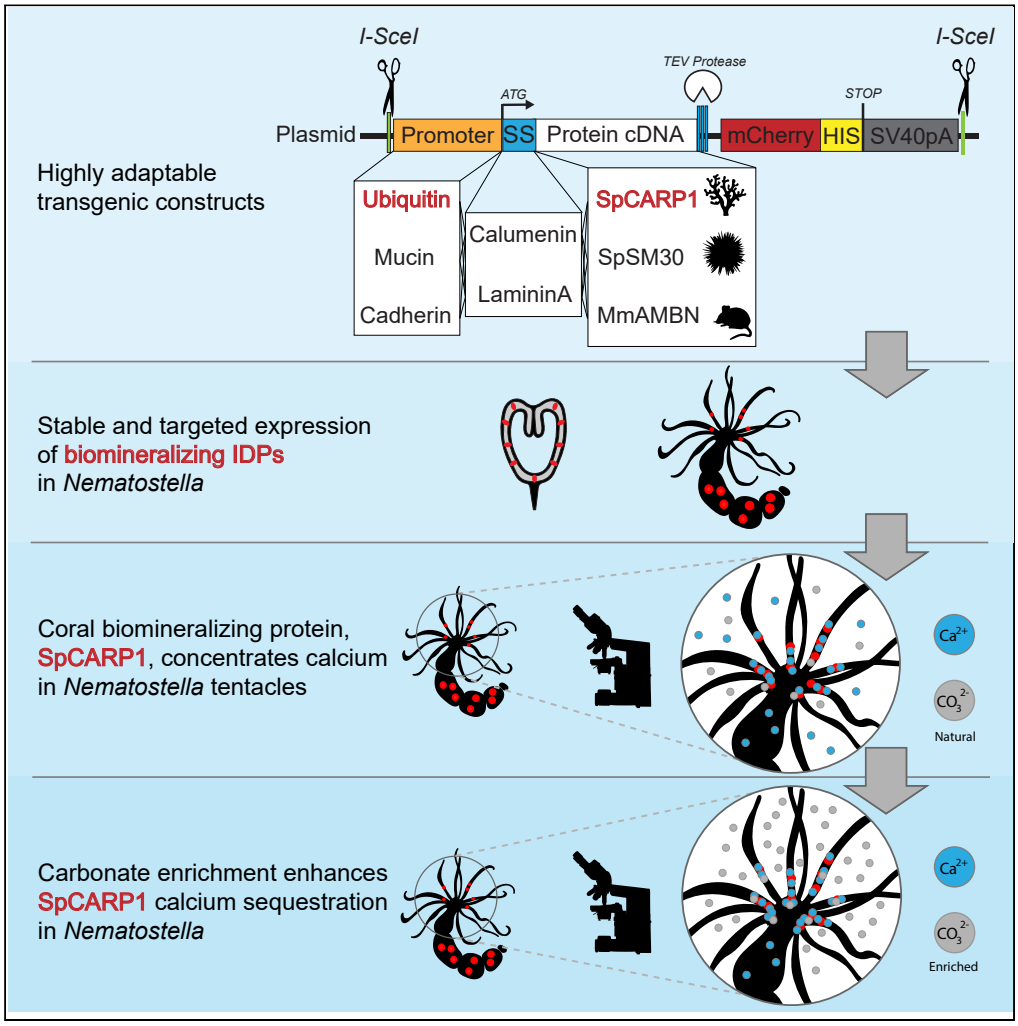


Brent Foster, Fredrik Hugosson, Federica Scucchia, Camille Enjolras, Leslie S. Babonis, William Hoaen, Mark Q. Martindale

brent.foster@whitney.ufl.edu (B.F.)
mqmartin@whitney.ufl.edu (M.Q.M.)

## Highlights

*Nematostella* is a tractable model to study cellular mechanisms of biomineralization

Transgenic constructs drive targeted and stable expression of biomineralizing IDPs

Coral biomineralizing IDP, SpCARP1, concentrates calcium ions in *Nematostella*

Carbonate enrichment enhances SpCARP1 calcium sequestration in *Nematostella*

Foster et al., iScience *27*, 109131
March 15, 2024 
https://doi.org/10.1016/j.isci.2024.109131

iScience

CellPress
OPEN ACCESS

Article

# A novel *in vivo* system to study coral biomineralization in the starlet sea anemone, *Nematostella vectensis*

Brent Foster,[1,*] Fredrik Hugosson,[1] Federica Scucchia,[1] Camille Enjolras,[1,2] Leslie S. Babonis,[1,3] William Hoaen,[4] and Mark Q. Martindale[1,5,*]

## SUMMARY

**Coral conservation requires a mechanistic understanding of how environmental stresses disrupt biomineralization, but progress has been slow, primarily because corals are not easily amenable to laboratory research. Here, we highlight how the starlet sea anemone, *Nematostella vectensis*, can serve as a model to interrogate the cellular mechanisms of coral biomineralization. We have developed transgenic constructs using biomineralizing genes that can be injected into *Nematostella* zygotes and designed such that translated proteins may be purified for physicochemical characterization. Using fluorescent tags, we confirm the ectopic expression of the coral biomineralizing protein, SpCARP1, in *Nematostella*. We demonstrate via calcein staining that SpCARP1 concentrates calcium ions in *Nematostella*, likely initiating the formation of mineral precursors, consistent with its suspected role in corals. These results lay a fundamental groundwork for establishing *Nematostella* as an *in vivo* system to explore the evolutionary and cellular mechanisms of coral biomineralization, improve coral conservation efforts, and even develop novel biomaterials.**

## INTRODUCTION

Coral reefs represent some of the most biodiverse ecosystems on Earth[1–3] and are necessary for maintaining healthy coastlines.[4,5] The backbone of these marine ecosystems are stony corals that, due to increased environmental stresses, are rapidly in decline.[6] Conservation efforts have been hampered, at least in part, by our limited understanding of the basic biology of corals and their ability to biomineralize and generate a diverse array of calcium carbonate skeletons that are susceptible to demineralization from changing ocean temperatures and acidification. Any meaningful effort to reverse the decline of corals requires a mechanistic understanding of 1) the molecular and biochemical processes of coral biomineralization and 2) how biomineralization is disrupted by environmental stresses. Unfortunately, efforts to probe the molecular basis of biomineralization in corals have proven difficult because of a general lack of genetic tools and difficulties culturing corals in laboratory settings.

Biomineralization is the production of inorganic minerals through biological mechanisms. This ability has evolved independently many times, resulting in unique structures such as bivalve shells,[7–10] sea urchin spicules,[10–14] and coral skeletons.[15–17] In marine organisms, the most studied mineralization pathways involve the absorption of $Ca^{2+}$[18,19] into cells expressing membrane-associated alpha carbonic anhydrases that convert $CO_2$ to bicarbonate.[20–23] This results in the production of amorphous calcium carbonate (ACC) precursors that are stabilized to form crystal structures secreted into the extracellular microenvironment.[24–27] ACC precursors attach to the growing surface of the coral skeleton and crystallize into aragonite under the control of highly acidic biomineralization proteins.[27,28] The acid-rich regions localize calcium ions, increasing the ionic strength within the calcification microenvironment.[29] These proteins, together with other molecules, behave as organic substrate that appears to serve as a nucleation site.[17]

Energetically favorable conditions for biomineralization can arise spontaneously and rapidly, suggestive of a mechanism by which ACC biomineralization could have evolved independently through the use of non-homologous proteins with similar physicochemical characteristics that result in similar mineralized materials.[24,27,30] Secreted proteins within mineralizing cells have been shown to catalyze nucleation[29,31] and/or interact with ACC precursors to provide stability as mineralizing tissue becomes more structured and complex.[13,27,32–34] These proteins are considered to be "intrinsically disordered" (IDP) because they have no set tertiary structures.[35–38] Although biomineralizing species

[1]The Whitney Laboratory for Marine Bioscience, Department of Biology, University of Florida, Gainesville, FL 32080, USA
[2]Institute of Human Genetics, CNRS, Montpellier 34090, France
[3]Department of Ecology and Evolutionary Biology, Cornell University, Ithaca, NY 14853, USA
[4]School of Biosciences, Cardiff University, Cardiff CF10 3AT, UK
[5]Lead contact
*Correspondence: brent.foster@whitney.ufl.edu (B.F.), mqmartin@whitney.ufl.edu (M.Q.M.)
https://doi.org/10.1016/j.isci.2024.109131

may not share homologous IDPs, many of these proteins contain similar properties such as highly acidic residues[8,39–42] and post-translational modifications that modify their folding and biomineralizing activity.[32,34,42–45]

Existing biomineralization models have distinct advantages and disadvantages.[32,44,45] Bacterial expression systems help clarify the role of carbonic anhydrases in biomineralization,[44–46] yet they are unable to modify proteins endogenously after translation and therefore cannot be used for elucidating the role of post-translational modifications in biomineralization. Eukaryotic cell cultures may be useful for testing the functional role of post-translational modifications of marine proteins, with the most success coming from mollusk nacre proteins expressed in insect lines.[47,48] However, to our knowledge, few groups have been able to establish stable cell cultures derived from marine invertebrates.[49,50] Existing cell lines rely on media that are not compatible with marine ecosystems, meaning any inferred insight into the evolutionary and biological mechanisms of biomineralization would need to be validated *in vivo* within a marine system. Marine invertebrates offer several advantages to *in vivo* assays of biomineralization. Sea urchins are useful as developmental models to understand the dynamics of spicule growth during embryonic skeleton formation[34,51] and syncytial mineralization.[52] Mollusks can be used to test the effects of novel, taxon-specific proteins on shell formation.[37,40] Corals are useful for characterizing how matrix proteins stabilize biominerals in extracellular microenvironments.[15,27] In each of these *in vivo* systems, mechanistic studies of the dynamic processes of biomineralization can be difficult to interpret due to the complexity of the interacting biomineralizing processes.[53]

Here, we present the starlet sea anemone (*Nematostella vectensis*) as a model for studying the dynamic processes of biomineralization. Despite being in the same class (Anthozoa) as scleractinian corals, *N. vectensis* does not naturally mineralize, eliminating potential confounding factors of interacting mineralization reactions.[53] Comparative genomics reveals that *N. vectensis* retains much of the molecular machinery believed to be necessary for biomineralization, including carbonic anhydrases as well as SpCARP1-related proteins such as Calumenin.[29,54] *N. vectensis* is a powerful developmental model that can easily produce thousands of embryos on demand with simple light and temperature cues. Many techniques for manipulating gene expression are already well established in N. vectensis, including CRISPR/Cas9 genome editing,[55–58] stable and transient cell-type-specific transgenesis,[59–62] and various forms of gene knockdown techniques (e.g., antisense morpholinos, RNAi, shRNA, dominant-negative approaches).[60,63,64] Together, these attributes make *N. vectensis* well-suited for investigating gene function during biomineralization.

In this article, we show that *N. vectensis* can express transgenic proteins involved in biomineralization in other taxa and present a novel *in vivo* system to evaluate the ability of IDPs to self-assemble into hierarchical structures to interact with calcium ions to further understand biomineralization.

## RESULTS

### Plasmid constructs are adaptable for targeted and stable transgenesis

*N. vectensis* embryos grow into swimming planulae within 48 h postfertilization (hpf), settle, then develop into small polyps in about a week when kept at room temperature (25°C) (Figure 1A). We also injected zygotes with a putative ubiquitin promoter driving the mCherry fluorescent signal and showed broad expression in planulae (Figures 1B and 1B′) and small polyps (Figures 1C and 1C′). We also designed plasmid vectors to incorporate other putative promoters endogenous to *N. vectensis*, as well as native signal sequences, driving the expression of IDPs involved in biomineralization (Figure 1D). We could not detect any visible difference between plasmid constructs containing signal sequences (SS) native to *N. vectensis* or those present in non-native cloned constructs. As such, the remainder of our data makes no distinction between whether constructs contain SS endogenous to *N. vectensis* or cloned sequences.

Animals injected with the constructs containing the ubiquitin promoter driving the expression of SpCARP1 exhibit transient expression as early as 24 hpf. Early developmental stages show higher expression of mCherry signal compared to later stages (Figure S1A). Calcein and mCherry signals appear to be most intense in primary polyps incubated in carbonate-enriched water (Figures S1B and S1C). By the planula stage, mCherry signal is broadly detected in both endoderm and ectoderm (Figure 2A). Expression expands into the body column and tentacles of developing small polyps (Figure 2B), with the strongest signal in scattered ectodermal cells (see arrows in Figures 2A and 2B, Figures S2A, S2B, S2C, and S2D). SpCARP1::mCherry signal persists when cells are dissociated (Figures S3A and S2B). Within 24 h of dissociation, cells form aggregate clumps and maintain fluorescent signal (Figures S3C and S2D). The mucin promoter drives the expression of SpCARP1 within 48 hpf in the aboral ectoderm of developing planulae in characteristic scattered secretory gland cells (Figure 2C). A strong mosaic signal expands into the body column and tentacles of small polyps in what appears to be glandular cells (Figure 2D; see arrows).

### SpCARP1 preferentially co-localizes with calcein in the tentacles of polyps

We imaged live transgenic polyps to observe the pattern of expression of SpCARP1 and the potential co-localization of the protein with calcium ions, suggestive of biomineralization-related activity. A limited calcein signal is also present in WT controls (Figures 3A–3F′), indicating that the fluorescent dye binds to calcium ions naturally present in the organism. In transgenic polyps, noticeable mCherry fluorescence is localized primarily at the tip of the tentacles and sparse regions along the tentacle cavity (Figures 3G–3I′; see white arrows). The mCherry signal is also present around the oral pole. Co-localization of calcein and mCherry fluorescence in the tentacles is evident in the endoderm of the tentacle cavity (Figures 3G–3I′) and in sparse regions surrounding the mouth (Figure 3H). Along the body and in the aboral end, the mCherry fluorescence is prevalent in the endoderm and the gastrovascular cavity, whereas the calcein signal is mostly localized to the ectoderm (Figures 3J–3L′). This pattern suggests that the calcium-binding activity of SpCARP1 is mostly concentrated in the tentacles of *N. vectensis* polyps.

*Nematostella* also harbors SpCARP1-related proteins such as Calumenins.[29,65] Previous phylogenetic analysis identified three protein sequences from the *Nematostella* genome that are closely related to SpCARP1.[29] These are partial protein sequences with a shared origin from

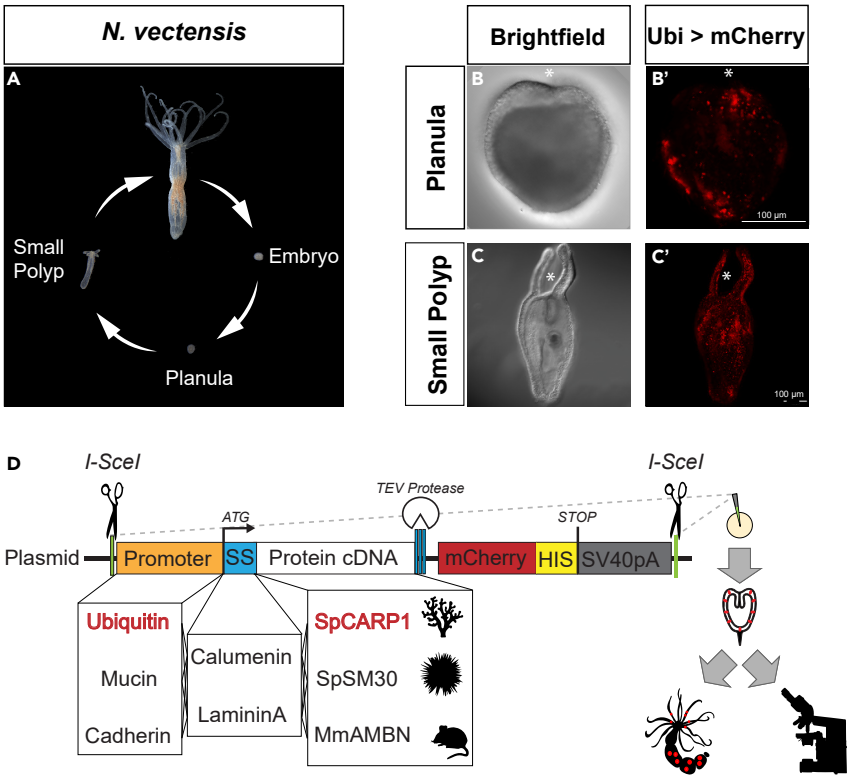


**Figure 1.** ***Putative promoters are sufficient to drive the stable expression of mCherry***

Life cycle of *N. vectensis* (A). Brightfield and Max projections showing the ubiquitin promoter driving the expression of mCherry in live planula (B–B′) and small polyps (C–C′). Plasmid construct containing native promoters, signal sequences (SS), and proteins involved in the biomineralization of coral (SpCARP1), sea urchin spicule (SpSM30), and mouse tooth enamel (MmAMBN), as well as the general workflow including microinjections, rearing of animals with incorporated transgene and evaluation of fluorescent mCherry signal with confocal microscopy (D). Asterisk = oral pole.

the full-length protein encoded by one gene, NVE221, which has been referred to as Calumenin F in previous literature[58,65] (see Figure S3). Here, we denote this SpCARP1-like protein as NvCaluF. The partial protein sequences included in Mass et al.[29] lack the N-terminal part of the full length NvCaluF protein encoded by NVE221 and were therefore not considered acidic such as SpCARP1. Our analysis of the full length NvCaluF protein sequence shows that it contains an exceptionally acidic N-terminal domain (see Figure S3; Table S1) characteristic of SpCARPs.[29]

### Artificially enriching seawater with carbonate enhances the SpCARP1 sequestration of calcium ions

We artificially enriched our seawater with carbonate and/or calcium ions to mimic the concentrated ionic conditions created by coral calcifying cells as they prepare for skeleton deposition. Incubation in carbonate-enriched seawater appears to increase expression in polyp tentacles, as indicated by the expanded expression of mCherry fluorescence in both the endoderm and ectoderm (Figures 4A–4C′). Such higher expression seems to be accompanied by a significant sequestration of calcium ions (pink reflects the overlap between mCherry and calcein signals in Figures 4A–4C′; see arrowheads). The body and aboral ends show a similar expression pattern to non-enriched conditions (see Figures 3J–3L′), with higher mCherry fluorescence in the endoderm and gastrovascular cavity and higher calcein signal in the ectoderm (Figures 4D–4F′), although some regions of overlapping mCherry-calcein fluorescence are present (see arrowhead in Figures 4E–4E′). A similar pattern can be observed in polyps with calcium-enriched seawater (Figures 5A–5F′), although the mCherry signal appears to be dimmer in these conditions compared to carbonate-only-enriched sea water (particularly in the tentacles; see Figures 5A–C′). When calcium ions are enriched, mCherry fluorescence is also observable in the ectoderm of the aboral region (Figures 5D–5F′) compared to just the endoderm of animals in non-enriched solutions (see Figures 3K–3K′). In addition, compared to the non-enriched conditions (Figures 3H–3I′), the mCherry signal along the endoderm of the tentacle is less sparse and more homogeneous when calcium ions are enriched (Figures 5B–5C′). Enriching seawater with both calcium and carbonate did not appear to affect the ability of SpCARP1 to sequester and concentrate calcium (Figure S4).

## DISCUSSION

We have demonstrated how *N. vectensis*, a soft-bodied anthozoan, may be utilized to study biomineralization *in vivo*.

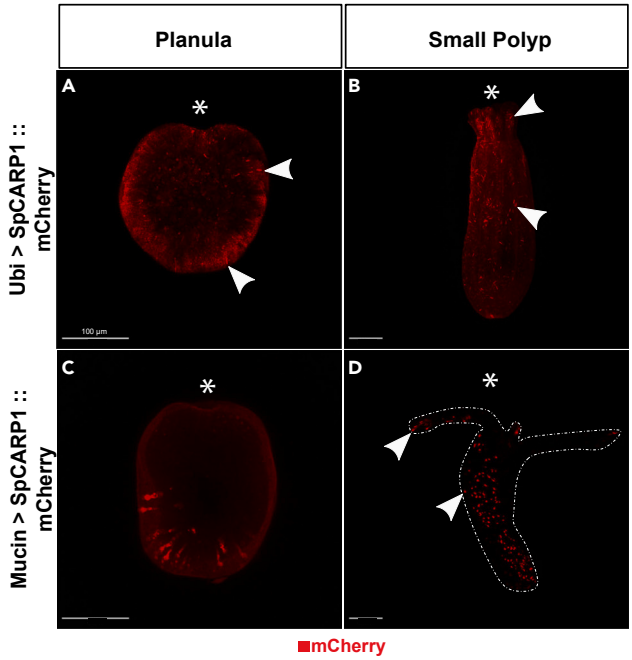


**Figure 2.** ***SpCARP1::mCherry expression can be driven by endogenous Nv promoters***

Ubiquitin promoter drives broad expression in ectoderm in live planulae (A) and small polyps (B), with the strongest signal in scattered ectodermal cells (see white arrowheads). Mucin promoter drives expression in secretory cells in fixed planula aboral ectoderm (C) and throughout the body column and tentacles of small polyps (D). Asterisk = oral pole. All scale bars = 100µm. See also Figures S1 and S2.

The putative promoters presented here were selected for optimizing the quantity and secretion of target biomineralization IDPs. Ubiquitin, as a regulatory protein that is highly conserved across eukaryotes, should be found in virtually every animal cell. Indeed, the *cis*-regulatory sequence we identified as a ubiquitin promoter appears to drive the broad expression of mCherry in a variety of cell types by 24 hpf (Figures 2A and 2B). Such selective expression could be due to an incomplete regulatory sequence or selective protein degradation. Our data shows the putative mucin promoter drives the expression of SpCARP1::mCherry within 48 hpf in secretory cells of the aboral ectoderm, with strong mosaic expression throughout the body column and into the tentacles of unfed polyps (Figures 2C and 2D), consistent with the expression of mucin.[66] Mucin-secreting cells are extremely abundant in the aboral ectoderm, and because these animals are excellent regenerators a stable transgenic line with the mucin promoter driving the expression of SpCARP1::mCherry should provide abundant material for future analyses of the interactions between SpCARP1 and putative IDPs.

Corals have specialized cells that control the chemistry of seawater in a confined space where skeleton deposition occurs, otherwise defined as the "calcifying space." Corals concentrate calcium and carbonate ions in this calcifying space, and IDPs such as SpCARP proteins control the nucleation of aragonite.[29] *N. vectensis*, as a non-calcifying organism, does not possess such specialized calcifying cells. By simulating the biomineralization-favorable conditions of high calcium and high carbonate concentrations, we were able to assess the responsiveness of SpCARP1 and detect regions within *N. vectensis* polyps where biomineralization may be most likely to occur. Analysis of the full length NvCaluF shows that it contains the characteristic acidic domain extension seen in SpCARP1 (Figure S3; Table S1). NvCaluF mRNA has been shown to be exclusively expressed in stinging cells in late planulae and early primary polyps via *in situ* hybridization.[58] This expression pattern is consistent with reports of SpCARP1 being located in the oral epidermis and in association with stinging cells in *S. pistillata* tentacles.[67] By supplementing our 1/3X FSW with calcium- and/or carbonate-rich solutions and evaluating calcium sequestration with calcein staining (Figures 3, 4, and 5; see also Figure S4), we show that the calcium-binding activity of SpCARP1 is primarily concentrated in the tentacles of *N. vectensis* polyps and seems to be enhanced with increased concentrations of carbonate ions in seawater (Figure 4), a critical requirement for biomineral nucleation. Our results are consistent with the initial stages of the formation of amorphous calcium carbonate and suggestive of a gradual self-assembly mechanism that concentrates calcium as a function of exogenous expression of SpCARP1 in *N. vectensis*. Future studies can further assess the presence of mineral structures in *N. vectensis* tentacles using scanning electron microscopy or polarized light optical microscopy.

We demonstrate that our experimental system is versatile and may be adapted to other forms of biomineralization. We show that *N. vectensis* can express IDPs involved in the $CaCO_3$ biomineralization of sea urchin spicules and $CaPO_4$ precipitation in vertebrate tooth enamel (Figure S5). The persistence of fluorescent signal in dissociated cells (Figure S3) suggests it should be possible to investigate the matrix-mediated polarization of IDPs and to test the role of intercellular interactions by taking advantage of 3D sculpting of dissociated transgenic *N. vectensis* cells. Given the amount of embryonic material provided in a single spawning cycle and the ease of injections, *N. vectensis*

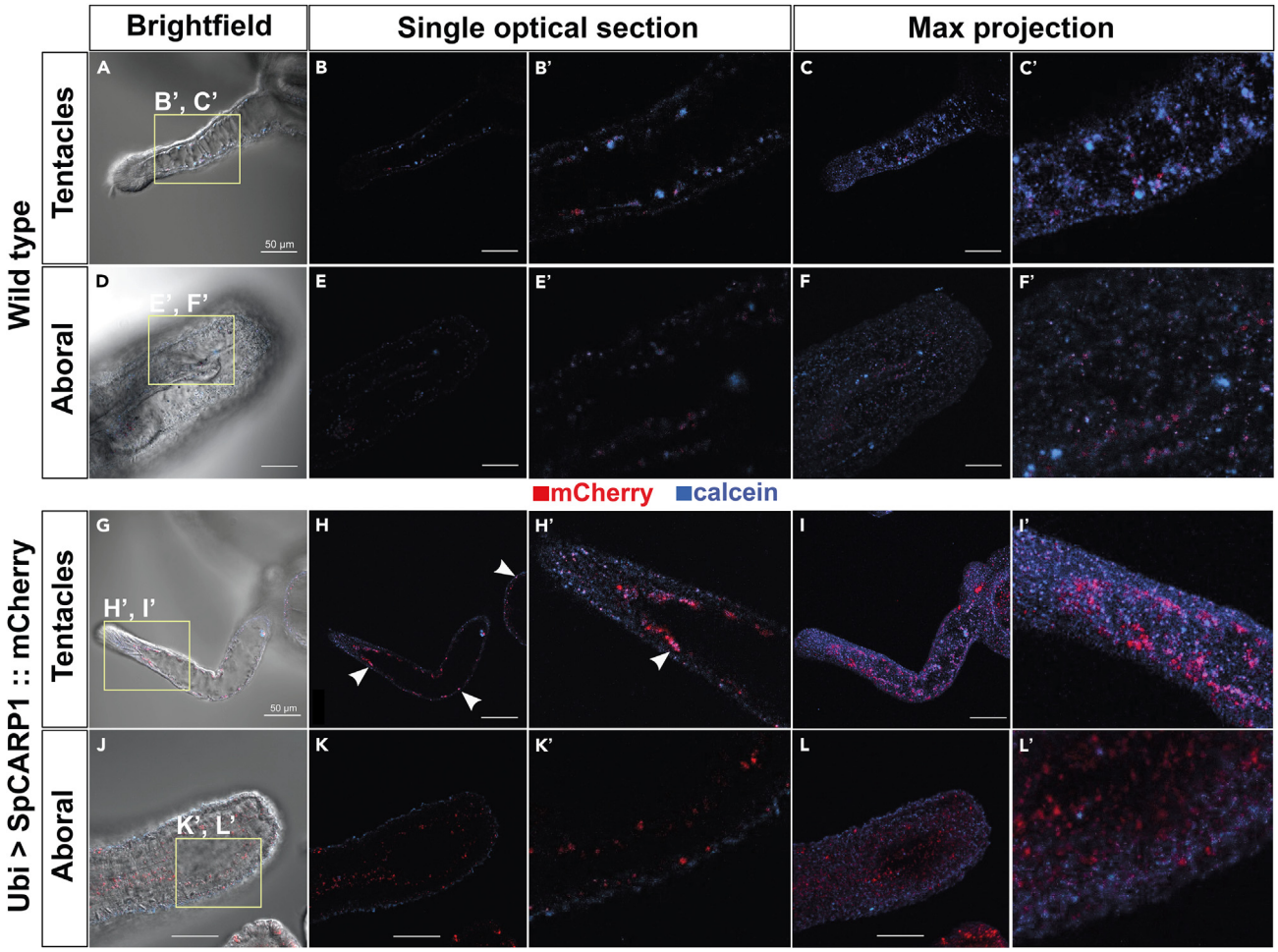


**Figure 3.** ***Calcein co-localizes with SpCARP1 in live polyp tentacles (unenriched seawater)***

Live uninjected polyps show limited calcein signal in tentacular (A–C′) and aboral (D–F′) regions. Live polyps injected with Ubi>SpCARP1::mCherry plasmid show the co-localization of calcein and mCherry signal in tentacular (G–I′) but not aboral (J–L′) regions. Arrowheads indicate co-localization of SpCARP1 with calcein stain. All scale bars = 50 µm. See also Figure S4.

may be used as an expression system to generate large amounts of cells expressing biomineralizing IDPs that can be isolated, purified, and assayed in controlled *in vitro* crystallization environments. In all, our results hint at the possibility to expand the use of the *N. vectensis* system to other forms of biomineralization and perhaps even develop novel biomineralized materials for biomedical research.

The primary focus of this study was to show how *N. vectensis* may be utilized to understand the molecular mechanisms that drive coral biomineralization to assist future conservation efforts. This study is the first to attempt to induce biological mineralization in a novel *in vivo* system. We chose the coral acidic protein SpCARP1 because it has been shown to induce rapid mineralization *in vitro*,[29] and to concentrate calcium ions leading to the formation of aragonite crystals in coral proto-polyps derived from cell cultures.[68] However, the calcium ion-concentration activity of such a protein has never been reported in live adult organisms, like we show here in *Nematostella* small polyps.

We demonstrate that *N. vectensis* can both tolerate the transgenic expression of intrinsically disordered proteins involved in biomineralization from a range of taxa that can sequester and concentrate calcium ions in a carbonate-enriched seawater solution, providing compelling evidence for the initiation of the biomineralizing process in a non-mineralizing organism. These results highlight the potential of *N. vectensis* in examining the capacity of various cell types to secrete biominerals, opening up opportunities to understand the capacity of cells to acquire novel functions. Our model system may be used as a proxy to coral systems in the lab to test the molecular components of biomineralization that may improve stress tolerance and resilience to native coral populations, thereby filling a much-needed gap in coral research and aiding restoration efforts.

## Limitations of the study

A single transgenic IDP is likely insufficient to lead to the formation of a mature skeleton. Nevertheless, this study lays the groundwork to establish *N. vectensis* as a tool to interrogate other coral IDPs, transporters, ion pumps, and so forth that are implicated in coral biomineralization and that can be co-expressed in the same or adjacent cell types *in vivo*. For example, another coral acid-rich protein, SpCARP4,

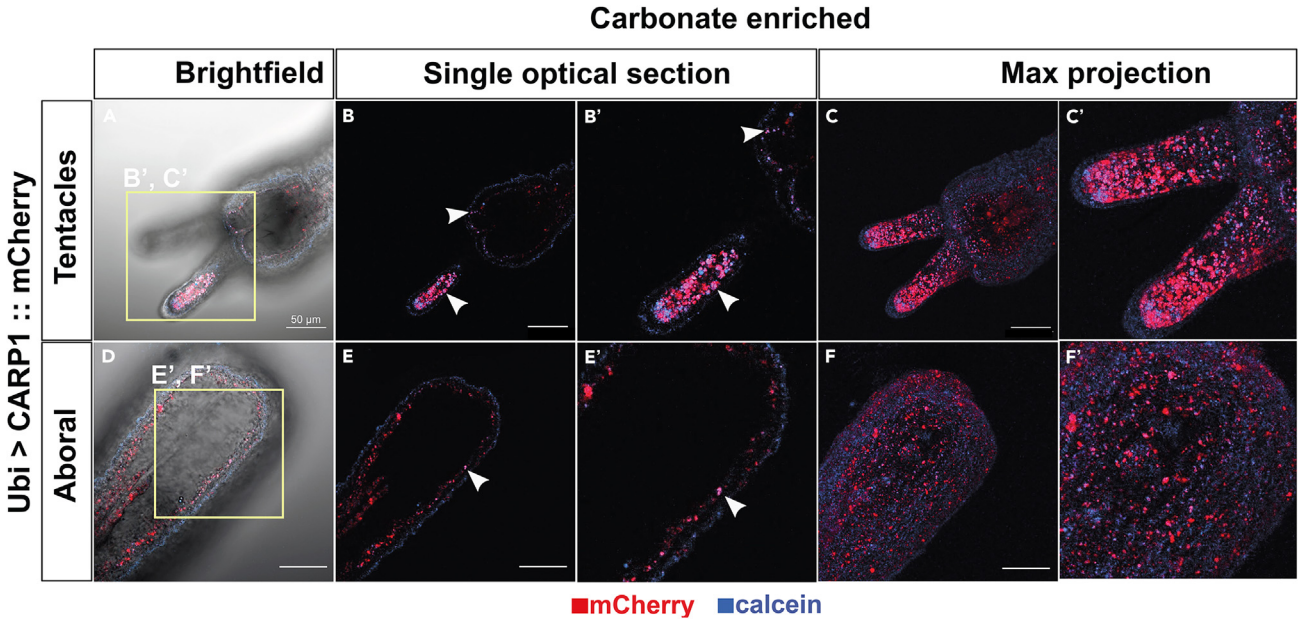


**Figure 4.** ***Carbonate-enriched seawater enhances the calcium sequestration of SpCARP1 in live polyps***

Tentacular (A–C′) and aboral (D–F′) views of live polyps following the incubation of carbonate-enriched seawater. White arrowheads indicate the co-localization of SpCARP1 with calcein stain. All scale bars = 50µm. See also Figure S4.

is of particular interest because it is one of the most abundant proteins in the coral skeleton and has been suggested to guide the formation of calcium carbonate crystals to specific orientations.[67] SpCARP4 is the most abundant protein in the coral skeletal organic matrix[54] that localizes with mineral nanoparticles in early mineralization zones, desmocytes (modified cells that anchor tissue to the skeleton), and oral epidermis.[67] The expression of SpCARP4 has also been detected in calicoblasts, the cells involved in the production of calcium carbonate.[69] We predict that *N. vectensis* will be able to tolerate SpCARP4 transgenesis and, if expressed together with SpCARP1, reveal new insights into the interaction between different IDPs and their respective functions in biomineralization. Future studies should evaluate whether *N. vectensis* produces the post-translational modifications on SpCARP1 believed to promote biomineralizing activity. Such experiments may be

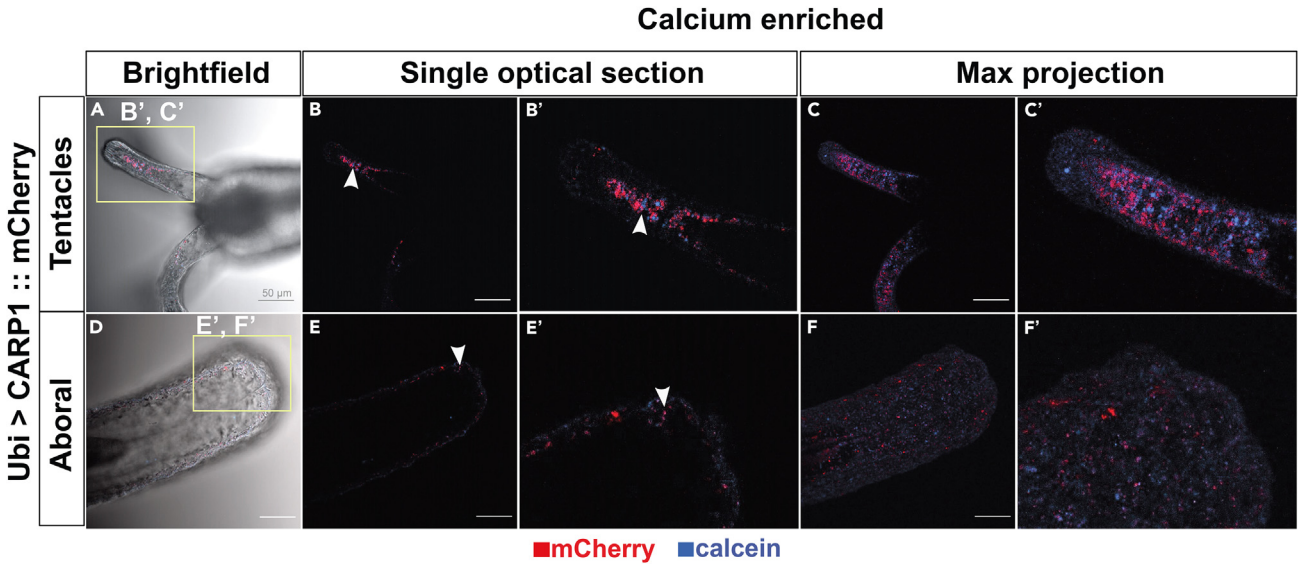


**Figure 5.** ***Calcium-enriched seawater does not improve the calcium-sequestration of SpCARP1 in live polyps***

Tentacular (A–C′) and aboral (D–F′) views of live transgenic polyps following the incubation of calcium-enriched seawater. White arrowheads show the co-localization of SpCARP1 with calcein stain. All scale bars = 50µm. See also Figure S4.

cross-checked with site-directed mutagenesis and biochemical analyses of modified proteins to clarify position-specific roles of post-translational modifications on biomineralizing activities. These studies may help delineate the mechanisms that led calcifying cells to evolve independently in many organisms from a patchwork of nonhomologous proteins and cellular pathways. Such mechanistic studies are necessary to understand how biomineralizing organisms have responded to environmental changes in the past and how they may respond in the future, thereby elucidating how $CaCO_3$ biomineralization shapes Earth's surface environment.[53,70–73]

## STAR★METHODS

Detailed methods are provided in the online version of this paper and include the following:

- KEY RESOURCES TABLE
- RESOURCE AVAILABILITY
  - Lead contact
  - Materials availability
  - Data and code availability
- METHOD DETAILS
  - Animal culture
  - Molecular cloning and in vitro mRNA transcription
  - Isolation of promoter DNA sequences
  - Generation of expression constructs for transgenesis
  - Microinjection
  - Fixation and confocal microscopy
  - Water enrichment and calcein incubation
  - Fluorescence intensity
  - Single cell dissociations
  - Analysis of protein sequences and their amino acid composition

## SUPPLEMENTAL INFORMATION

Supplemental information can be found online at https://doi.org/10.1016/j.isci.2024.109131.

## ACKNOWLEDGMENTS

This research was funded by NSF grant # IOS 2314456.

## AUTHOR CONTRIBUTIONS

Conceptualization, B.F. F.H., F.S., C.E., and M.Q.M; methodology, B.F., F.H., F.S. C.E., L.S.B., and M.Q.M.; validation, B.F., F.H., F.S., and C.E.; formal analysis, B.F., F.H., and F.S.; investigation, B.F., F.H., F.S., C.E., and W.H.; resources, B.F., F.H., F.S., and C.E.; data curation, B.F., F.H, F.S., and C.E.; writing – original draft, B.F.; writing – review and editing, B.F, F.H., F.S., C.E., L.S.B., and M.Q.M.; visualization, B.F., F.H, and F.S.; supervision, F.H. and M.Q.M.; project administration, F.H. and M.Q.M.; funding acquisition, M.Q.M.

## DECLARATION OF INTERESTS

The authors declare no competing interests.

Received: October 20, 2023
Revised: December 18, 2023
Accepted: February 1, 2024
Published: February 6, 2024

## REFERENCES

1. Reaka-Kudla, M.L. (1997). In Biodiversity II: Understanding and Protecting Our Biological Resources, M.L. Reaka-Kudla, D.E. Wilson, and E.O. Wilson, eds. (Joseph Henry Press).
2. Small, A., Adey, W.H., and Spoon, D. (1998). Are Current Estimates of Coral Reef Biodiversity Too Low? the View through the Window of a Microcosm. Atoll Res. Bull. *458*, 1–20. https://doi.org/10.5479/SI.00775630.458.1.
3. Wagner, D., Friedlander, A.M., Pyle, R.L., Brooks, C.M., Gjerde, K.M., and Wilhelm, T.'. (2020). Coral Reefs of the High Seas: Hidden Biodiversity Hotspots in Need of Protection. Front. Mar. Sci. *7*, 567428. https://doi.org/10.3389/FMARS.2020.567428/BIBTEX.
4. Arkema, K.K., Guannel, G., Verutes, G., Wood, S.A., Guerry, A., Ruckelshaus, M., Kareiva, P., Lacayo, M., and Silver, J.M. (2013). Coastal habitats shield people and property from sea-level rise and storms. Nat. Clim. Chang. *3*, 913–918. https://doi.org/10.1038/NCLIMATE1944.
5. Moberg, F., and Folke, C. (1999). Ecological goods and services of coral reef ecosystems. Ecol. Econ. *29*, 215–233. https://doi.org/10.1016/S0921-8009(99)00009-9.
6. Baker, A.C., Glynn, P.W., and Riegl, B. (2008). Climate change and coral reef bleaching: An ecological assessment of long-term impacts, recovery trends and future outlook. Estuar.

Coast. Shelf Sci. *80*, 435–471. https://doi.org/10.1016/J.ECSS.2008.09.003.
7. Addadi, L., Joester, D., Nudelman, F., and Weiner, S. (2006). Mollusk Shell Formation: A Source of New Concepts for Understanding Biomineralization Processes. Chem Eur J *12*, 980–987. https://doi.org/10.1002/chem.200500980.
8. Gotliv, B.A., Addadi, L., and Weiner, S. (2003). Mollusk Shell Acidic Proteins: In Search of Individual Functions. Chembiochem. *4*, 522–529. https://doi.org/10.1002/CBIC.200200548.
9. Marie, B., Joubert, C., Tayalé, A., Zanella-Cléon, I., Belliard, C., Piquemal, D., Cochennec-Laureau, N., Marin, F., Gueguen, Y., and Montagnani, C. (2012). Different secretory repertoires control the biomineralization processes of prism and nacre deposition of the pearl oyster shell. Proc Natl Acad Sci USA *109*, 20986-91. https://doi.org/10.1073/pnas.1210552109.
10. Weiner, S. (2008). Biomineralization: A structural perspective. J. Struct. Biol. *163*, 229–234. https://doi.org/10.1016/J.JSB.2008.02.001.
11. Decker, G.L., Morrill, J.B., and Lennarz, W.J. (1987). Characterization of sea urchin primary mesenchyme cells and spicules during biomineralization in vitro. Development *101*, 297–312. https://doi.org/10.1242/DEV.101.2.297.
12. Gildor, T., Winter, M.R., Layous, M., Hijaze, E., and Ben-Tabou de-Leon, S. (2021). The biological regulation of sea urchin larval skeletogenesis – From genes to biomineralized tissue. J. Struct. Biol. *213*, 107797.
13. Politi, Y., Arad, T., Klein, E., Weiner, S., and Addadi, L. (2004). Sea Urchin Spine Calcite Forms via a Transient Amorphous Calcium Carbonate Phase. New Ser *306*, 1161–1164.
14. Seto, J., Ma, Y., Davis, S.A., Meldrum, F., Gourrier, A., Kim, Y.-Y., Schilde, U., Sztucki, M., Burghammer, M., Maltsev, S., et al. (2012). Structure-property relationships of a biological mesocrystal in the adult sea urchin spine. Proc. Natl. Acad. Sci. USA *109*, 3699–3704. https://doi.org/10.1073/pnas.1109243109.
15. Mor Khalifa, G., Levy, S., and Mass, T. (2021). The calcifying interface in a stony coral primary polyp: An interplay between seawater and an extracellular calcifying space. J. Struct. Biol. *213*, 107803. https://doi.org/10.1016/j.jsb.2021.107803.
16. Neder, M., Laissue, P.P., Akiva, A., Akkaynak, D., Albéric, M., Spaeker, O., Politi, Y., Pinkas, I., and Mass, T. (2019). Mineral formation in the primary polyps of pocilloporoid corals. Acta Biomater. *96*, 631–645. https://doi.org/10.1016/j.actbio.2019.07.016.
17. Von Euw, S., Zhang, Q., Manichev, V., Murali, N., Gross, J., Feldman, L.C., Gustafsson, T., Flach, C., Mendelsohn, R., and Falkowski, P.G. (2017). Biological control of aragonite formation in stony corals. Science *356*, 933–938. https://doi.org/10.1126/SCIENCE.AAM6371.
18. Kahil, K., Varsano, N., Sorrentino, A., Pereiro, E., Rez, P., Weiner, S., and Addadi, L. (2020). Cellular pathways of calcium transport and concentration toward mineral formation in sea urchin larvae. Proc. Natl. Acad. Sci. USA *117*, 30957–30965. https://doi.org/10.1073/PNAS.1918195117.
19. Kahil, K., Weiner, S., Addadi, L., and Gal, A. (2021). Ion Pathways in Biomineralization: Perspectives on Uptake, Transport, and Deposition of Calcium, Carbonate, and Phosphate. J. Am. Chem. Soc. *143*, 21100–21112. https://doi.org/10.1021/jacs.1c09174.
20. Bose, H., and Satyanarayana, T. (2017). Microbial Carbonic Anhydrases in Biomimetic Carbon Sequestration for Mitigating Global Warming: Prospects and Perspectives. Front. Microbiol. *8*, 1615. https://doi.org/10.3389/FMICB.2017.01615.
21. Le Roy, N., Jackson, D.J., Marie, B., Ramos-Silva, P., and Marin, F. (2014). The evolution of metazoan aα-carbonic anhydrases and their roles in calcium carbonate biomineralization. Front. Zool. *11*, 1–16. https://doi.org/10.1186/S12983-014-0075-8/FIGURES/6.
22. Moya, A., Tambutté, S., Bertucci, A., Tambutté, E., Lotto, S., Vullo, D., Supuran, C.T., Allemand, D., and Zoccola, D. (2008). Carbonic Anhydrase in the Scleractinian Coral Stylophora pistillata: CHARACTERIZATION, LOCALIZATION, AND ROLE IN BIOMINERALIZATION. J. Biol. Chem. *283*, 25475–25484. https://doi.org/10.1074/JBC.M804726200.
23. Voigt, O., Adamski, M., Sluzek, K., and Adamska, M. (2014). Calcareous sponge genomes reveal complex evolution of α-carbonic anhydrases and two key biomineralization enzymes. BMC Evol. Biol. *14*, 1–19. https://doi.org/10.1186/S12862-014-0230-Z/FIGURES/6.
24. Addadi, L., Raz, S., and Weiner, S. (2003). Taking advantage of disorder: Amorphous calcium carbonate and its roles in biomineralization. Adv. Mater. *15*, 959–970. https://doi.org/10.1002/ADMA.200300381.
25. Nebel, H., Neumann, M., Mayer, C., and Epple, M. (2008). On the Structure of Amorphous Calcium Carbonate—A Detailed Study by Solid-State NMR Spectroscopy. Inorg. Chem. *47*, 7874–7879. https://doi.org/10.1021/ic8007409.
26. Whiticar, M.J., Suess, E., Wefer, G., and Müller, P.J. (2022). Calcium Carbonate Hexahydrate (Ikaite): History of Mineral Formation as Recorded by Stable Isotopes. Minerals *12*, 1627. https://doi.org/10.3390/min12121627.
27. Mass, T., Giuffre, A.J., Sun, C.Y., Stifler, C.A., Frazier, M.J., Neder, M., Tamura, N., Stan, C.V., Marcus, M.A., and Gilbert, P.U.P.A. (2017). Amorphous calcium carbonate particles form coral skeletons. Proc. Natl. Acad. Sci. USA *114*, E7670–E7678. https://doi.org/10.1073/PNAS.1707890114.
28. Laipnik, R., Bissi, V., Sun, C.-Y., Falini, G., Gilbert, P.U.P.A., and Mass, T. (2020). Coral acid rich protein selects vaterite polymorph in vitro. J. Struct. Biol. *209*, 107431. https://doi.org/10.1016/j.jsb.2019.107431.
29. Mass, T., Drake, J.L., Haramaty, L., Kim, J.D., Zelzion, E., Bhattacharya, D., and Falkowski, P.G. (2013). Cloning and characterization of four novel coral acid-rich proteins that precipitate carbonates in vitro. Curr. Biol. *23*, 1126–1131. https://doi.org/10.1016/j.cub.2013.05.007.
30. Gower, L.B., and Odom, D.J. (2000). Deposition of calcium carbonate films by a polymer-induced liquid-precursor (PILP) process. J. Cryst. Growth *210*, 719–734. https://doi.org/10.1016/S0022-0248(99)00749-6.
31. George, A., Sabsay, B., Simonian, P.A., and Veis, A. (1993). Characterization of a Novel Dentin Matrix Acidic Phosphoprotein IMPLICATIONS FOR INDUCTION OF BIOMINERALIZATION. J. Biol. Chem. *268*, 12624–12630. https://doi.org/10.1016/S0021-9258(18)31434-0.
32. Helman, Y., Natale, F., Sherrell, R.M., LaVigne, M., Starovoytov, V., Gorbunov, M.Y., and Falkowski, P.G. (2008). Extracellular matrix production and calcium carbonate precipitation by coral cells in vitro. Proc. Natl. Acad. Sci. USA *105*, 54–58. https://doi.org/10.1073/PNAS.0710604105.
33. Veis, A., and Dorvee, J.R. (2013). Biomineralization mechanisms: A new paradigm for crystal nucleation in organic matrices. Calcif. Tissue Int. *93*, 307–315. https://doi.org/10.1007/S00223-012-9678-2/FIGURES/4.
34. Wilt, F.H., Killian, C.E., Hamilton, P., and Croker, L. (2008). The dynamics of secretion during sea urchin embryonic skeleton formation. Exp. Cell Res. *314*, 1744–1752. https://doi.org/10.1016/j.yexcr.2008.01.036.
35. Kalmar, L., Homola, D., Varga, G., and Tompa, P. (2012). Structural disorder in proteins brings order to crystal growth in biomineralization. Bone *51*, 528–534. https://doi.org/10.1016/J.BONE.2012.05.009.
36. Moradian-Oldak, J., and George, A. (2021). Biomineralization of Enamel and Dentin Mediated by Matrix Proteins. J. Dent. Res. *100*, 1020–1029. https://doi.org/10.1177/00220345211018405.
37. Ndao, M., Keene, E., Amos, F.F., Rewari, G., Ponce, C.B., Estroff, L., and Evans, J.S. (2010). Intrinsically disordered mollusk shell prismatic protein that modulates calcium carbonate crystal growth. Biomacromolecules *11*, 2539–2544. https://doi.org/10.1021/bm100738r.
38. Rose-Martel, M., Smiley, S., and Hincke, M.T. (2015). Novel identification of matrix proteins involved in calcitic biomineralization. J. Proteomics *116*, 81–96.
39. Gorski, J.P. (1992). Calcified Tissue International Acidic Phosphoproteins from Bone Matrix: A Structural Rationalization of Their Role in Biomineralization. Calcif. Tissue Int. *50*, 391–396.
40. Gotliv, B.A., Kessler, N., Sumerel, J.L., Morse, D.E., Tuross, N., Addadi, L., and Weiner, S. (2005). Asprich: A novel aspartic acid-rich protein family from the prismatic shell matrix of the bivalve Atrina rigida. Chembiochem. *6*, 304–314. https://doi.org/10.1002/CBIC.200400221.
41. Moradian-Oldak, J., Frolow, F., Addadi, L., and Weiner, S. (1992). Interactions between acidic matrix macromolecules and calcium phosphate ester crystals: relevance to carbonate apatite formation in biomineralization. Proc. Biol. Sci. *247*, 47–55. https://doi.org/10.1098/RSPB.1992.0008.
42. Suzuki, M., Saruwatari, K., Kogure, T., Yamamoto, Y., Nishimura, T., Kato, T., and Nagasawa, H. (2009). An Acidic Matrix Protein, Pif, Is a Key Macromolecule for Nacre Formation. Science *325*, 1388-90. https://doi.org/10.1126/science.1173793.
43. Kabakoff, B., Hwang, S.P., and Lennarz, W.J. (1992). Characterization of post-translational modifications common to three primary mesenchyme cell-specific glycoproteins involved in sea urchin embryonic skeleton formation. Dev. Biol. *150*, 294–305. https://doi.org/10.1016/0012-1606(92)90243-A.
44. Li, W., Liu, L., Chen, W., Yu, L., Li, W., and Yu, H. (2010). Calcium carbonate precipitation and crystal morphology induced by microbial carbonic anhydrase and other biological factors. Process Biochem. *45*, 1017–1021.

https://doi.org/10.1016/j.procbio.2010.03.004.
45. Smith, K.S., and Ferry, J.G. (2000). Prokaryotic carbonic anhydrases. FEMS Microbiol. Rev. *24*, 335–366. https://doi.org/10.1111/j.1574-6976.2000.tb00546.x.
46. Dhami, N.K., Reddy, M.S., and Mukherjee, A. (2014). Synergistic role of bacterial urease and carbonic anhydrase in carbonate mineralization. Appl. Biochem. Biotechnol. *172*, 2552–2561. https://doi.org/10.1007/S12010-013-0694-0/FIGURES/4.
47. Lim, S., Kim, K.R., Choi, Y.S., Kim, D.-K., Hwang, D., and Cha, H.J. (2011). In vivo post-translational modifications of recombinant mussel adhesive protein in insect cells. Biotechnol. Prog. *27*, 1390–1396. https://doi.org/10.1002/btpr.662.
48. Chang, E.P., Perovic, I., Rao, A., Cölfen, H., and Evans, J.S. (2016). Insect Cell Glycosylation and Its Impact on the Functionality of a Recombinant Intracrystalline Nacre Protein, AP24. Biochemistry *55*, 1024–1035. https://doi.org/10.1021/acs.biochem.5b01186.
49. Cai, X., and Zhang, Y. (2014). Marine invertebrate cell culture: a decade of development. J. Oceanogr. *70*, 405–414. https://doi.org/10.1007/s10872-014-0242-8.
50. Potts, R.W.A., Gutierrez, A.P., Cortés-Araya, Y., Houston, R.D., and Bean, T.P. (2020). Developments in marine invertebrate primary culture reveal novel cell morphologies in the model bivalve Crassostrea gigas. PeerJ *8*, e9180. https://doi.org/10.7717/peerj.9180.
51. Ettensohn, C.A., and Malinda, K.M. (1993). Size regulation and morphogenesis: A cellular analysis of skeletogenesis in the sea urchin embryo. Development *119*, 155–167. https://doi.org/10.1242/DEV.119.1.155.
52. Beniash, E., Addadi, L., and Weiner, S. (1999). Cellular Control Over Spicule Formation in Sea Urchin Embryos: A Structural Approach. J. Struct. Biol. *125*, 50–62. https://doi.org/10.1006/JSBI.1998.4081.
53. Clark, M.S. (2020). Molecular mechanisms of biomineralization in marine invertebrates. J. Exp. Biol. *223*, jeb206961. https://doi.org/10.1242/JEB.206961/223537.
54. Wang, X., Zoccola, D., Liew, Y.J., Tambutte, E., Cui, G., Allemand, D., Tambutte, S., and Aranda, M. (2021). The Evolution of Calcification in Reef-Building Corals. Mol. Biol. Evol. *38*, 3543–3555. https://doi.org/10.1093/MOLBEV/MSAB103.
55. Ikmi, A., McKinney, S.A., Delventhal, K.M., and Gibson, M.C. (2014). TALEN and CRISPR/Cas9-mediated genome editing in the early-branching metazoan Nematostella vectensis. Nat. Commun. *5*, 5486. https://doi.org/10.1038/ncomms6486.
56. Servetnick, M.D., Steinworth, B., Babonis, L.S., Simmons, D., Salinas-Saavedra, M., and Martindale, M.Q. (2017). Cas9-mediated excision of Nematostella brachyury disrupts endoderm development, pharynx formation and oral-aboral patterning. Development *144*, 2951–2960. https://doi.org/10.1242/dev.145839.
57. Nakanishi, N., and Martindale, M.Q. (2018). CRISPR knockouts reveal an endogenous role for ancient neuropeptides in regulating developmental timing in a sea anemone. eLife *7*, e39742. https://doi.org/10.7554/eLife.39742.
58. Babonis, L.S., Enjolras, C., Reft, A.J., Foster, B.M., Hugosson, F., Ryan, J.F., Daly, M., and Martindale, M.Q. (2023). Single-cell atavism reveals an ancient mechanism of cell type diversification in a sea anemone. Nat. Commun. *14*, 885. https://doi.org/10.1038/s41467-023-36615-9.
59. Renfer, E., and Technau, U. (2017). Meganuclease-assisted generation of stable transgenics in the sea anemone Nematostella vectensis. Nat. Protoc. *12*, 1844–1854. https://doi.org/10.1038/nprot.2017.075.
60. Layden, M.J., Röttinger, E., Wolenski, F.S., Gilmore, T.D., and Martindale, M.Q. (2013). Microinjection of mRNA or morpholinos for reverse genetic analysis in the starlet sea anemone, Nematostella vectensis. Nat. Protoc. *8*, 924–934. https://doi.org/10.1038/nprot.2013.009.
61. Richards, G.S., and Rentzsch, F. (2015). Regulation of Nematostella neural progenitors by SoxB, Notch and bHLH genes. Dev. Camb. Engl. *142*, 3332–3342. https://doi.org/10.1242/DEV.123745.
62. Renfer, E., Amon-Hassenzahl, A., Steinmetz, P.R.H., and Technau, U. (2010). A muscle-specific transgenic reporter line of the sea anemone, Nematostella vectensis. Proc. Natl. Acad. Sci. USA *107*, 104–108. https://doi.org/10.1073/pnas.0909148107.
63. He, S., del Viso, F., Chen, C.-Y., Ikmi, A., Kroesen, A.E., and Gibson, M.C. (2018). An axial Hox code controls tissue segmentation and body patterning in Nematostella vectensis. Science *361*, 1377–1380. https://doi.org/10.1126/science.aar8384.
64. Karabulut, A., He, S., Chen, C.-Y., McKinney, S.A., and Gibson, M.C. (2019). Electroporation of short hairpin RNAs for rapid and efficient gene knockdown in the starlet sea anemone, Nematostella vectensis. Dev. Biol. *448*, 7–15. https://doi.org/10.1016/j.ydbio.2019.01.005.
65. Ganot, P., Moya, A., Magnone, V., Allemand, D., Furla, P., and Sabourault, C. (2011). Adaptations to Endosymbiosis in a Cnidarian-Dinoflagellate Association: Differential Gene Expression and Specific Gene Duplications. PLoS Genet. *7*, e1002187. https://doi.org/10.1371/journal.pgen.1002187.
66. Steinmetz, P.R.H., Aman, A., Kraus, J.E.M., and Technau, U. (2017). Gut-like ectodermal tissue in a sea anemone challenges germ layer homology. Nat. Ecol. Evol. *1*, 1535–1542. https://doi.org/10.1038/s41559-017-0285-5.
67. Mass, T., Drake, J.L., Peters, E.C., Jiang, W., and Falkowski, P.G. (2014). Immunolocalization of skeletal matrix proteins in tissue and mineral of the coral Stylophora pistillata. Proc. Natl. Acad. Sci. USA *111*, 12728–12733. https://doi.org/10.1073/PNAS.1408621111/-/DCSUPPLEMENTAL.
68. Mass, T., Drake, J.L., Heddleston, J.M., and Falkowski, P.G. (2017). Nanoscale Visualization of Biomineral Formation in Coral Proto-Polyps. Curr Biol *27*, 3191–3196.e3. https://doi.org/10.1016/j.cub.2017.09.012.
69. Levy, S., Elek, A., Grau-Bové, X., Menéndez-Bravo, S., Iglesias, M., Tanay, A., Mass, T., and Sebé-Pedrós, A. (2021). A stony coral cell atlas illuminates the molecular and cellular basis of coral symbiosis, calcification, and immunity. Cell *184*, 2973–2987.e18. https://doi.org/10.1016/J.CELL.2021.04.005.
70. Drake, J.L., Mass, T., Stolarski, J., Von Euw, S., van de Schootbrugge, B., and Falkowski, P.G. (2020). How corals made rocks through the ages. Glob. Chang. Biol. *26*, 31–53. https://doi.org/10.1111/GCB.14912.
71. Gilbert, P.U.P.A., Bergmann, K.D., Boekelheide, N., Tambutté, S., Mass, T., Marin, F., Adkins, J.F., Erez, J., Gilbert, B., Knutson, V., et al. (2022). Biomineralization: Integrating mechanism and evolutionary history. Sci. Adv. *8*, eabl9653. https://doi.org/10.1126/SCIADV.ABL9653.
72. Hönisch, B., Ridgwell, A., Schmidt, D.N., Thomas, E., Gibbs, S.J., Sluijs, A., Zeebe, R., Kump, L., Martindale, R.C., Greene, S.E., et al. (2012). The geological record of ocean acidification. Science *335*, 1058–1063. https://doi.org/10.1126/SCIENCE.1208277.
73. Kawahata, H., Fujita, K., Iguchi, A., Inoue, M., Iwasaki, S., Kuroyanagi, A., Maeda, A., Manaka, T., Moriya, K., Takagi, H., et al. (2019). Perspective on the response of marine calcifiers to global warming and ocean acidification—Behavior of corals and foraminifera in a high CO2 world "hot house.". Prog. Earth Planet. Sci. *6*, 5–37. https://doi.org/10.1186/S40645-018-0239-9.
74. Hand, C., and Uhlinger, K.R. (1992). The Culture, Sexual and Asexual Reproduction, and Growth of the Sea Anemone Nematostella vectensis. Biol. Bull. *182*, 169–176. https://doi.org/10.2307/1542110.
75. Fritzenwanker, J.H., and Technau, U. (2002). Induction of gametogenesis in the basal cnidarian Nematostella vectensis(Anthozoa). Dev. Genes Evol. *212*, 99–103. https://doi.org/10.1007/S00427-002-0214-7.
76. Chin, J.X., Chung, B.K.S., and Lee, D.Y. (2014). Codon Optimization OnLine (COOL): A web-based multi-objective optimization platform for synthetic gene design. Bioinformatics *30*, 2210–2212. https://doi.org/10.1093/bioinformatics/btu192.
77. Kõressaar, T., Lepamets, M., Kaplinski, L., Raime, K., Andreson, R., and Remm, M. (2018). Primer3_masker: integrating masking of template sequence with primer design software. Bioinforma. Oxf. Engl. *34*, 1937–1938. https://doi.org/10.1093/BIOINFORMATICS/BTY036.
78. Hernández, G., Osnaya, V.G., and Pérez-Martínez, X. (2019). Conservation and Variability of the AUG Initiation Codon Context in Eukaryotes. Trends Biochem. Sci. *44*, 1009–1021. https://doi.org/10.1016/j.tibs.2019.07.001.
79. Waldo, G.S., Standish, B.M., Berendzen, J., and Terwilliger, T.C. (1999). Rapid protein-folding assay using green fluorescent protein. Nat. Biotechnol. *17*, 691–695. https://doi.org/10.1038/10904.
80. Almagro Armenteros, J.J., Tsirigos, K.D., Sønderby, C.K., Petersen, T.N., Winther, O., Brunak, S., von Heijne, G., and Nielsen, H. (2019). SignalP 5.0 improves signal peptide predictions using deep neural networks. Nat. Biotechnol. *37*, 420–423. https://doi.org/10.1038/s41587-019-0036-z.
81. Putnam, N.H., Srivastava, M., Hellsten, U., Dirks, B., Chapman, J., Salamov, A., Terry, A., Shapiro, H., Lindquist, E., Kapitonov, V.V., et al. (2007). Sea anemone genome reveals ancestral eumetazoan gene repertoire and genomic organization. Science *317*, 86–94. https://doi.org/10.1126/SCIENCE.1139158.
82. Marlow, H.Q., Srivastava, M., Matus, D.Q., Rokhsar, D., and Martindale, M.Q. (2009). Anatomy and development of the nervous system of Nematostella vectensis, an anthozoan cnidarian. Dev. Neurobiol. *69*, 235–254. https://doi.org/10.1002/dneu.20698.
83. Marlow, H., Roettinger, E., Boekhout, M., and Martindale, M.Q. (2012). Functional roles of Notch signaling in the cnidarian

Nematostella vectensis. Dev. Biol. *362*, 295–308. https://doi.org/10.1016/J.YDBIO.2011.11.012.

84. Schindelin, J., Arganda-Carreras, I., Frise, E., Kaynig, V., Longair, M., Pietzsch, T., Preibisch, S., Rueden, C., Saalfeld, S., Schmid, B., et al. (2012). Fiji: an open-source platform for biological-image analysis. Nat. Methods *9*, 676–682. https://doi.org/10.1038/nmeth.2019.
85. Pierrot, D., Lewis, E., and Wallace, D. (2006). MS Excel Program Developed for CO2 System Calculations. https://marine.gov.scot/sma/content/ms-excel-program-developed-co2-system-calculations.
86. Mehrbach, C., Culberson, C.H., Hawley, J.E., and Pytkowicx, R.M. (1973). MEASUREMENT OF THE APPARENT DISSOCIATION CONSTANTS OF CARBONIC ACID IN SEAWATER AT ATMOSPHERIC PRESSURE1. Limnol. Oceanogr. *18*, 897–907. https://doi.org/10.4319/LO.1973.18.6.0897.
87. Dickson, A.G., and Millero, F.J. (1987). A comparison of the equilibrium constants for the dissociation of carbonic acid in seawater media. Deep Sea Res. Part Oceanogr. Res. Pap. *34*, 1733–1743. https://doi.org/10.1016/0198-0149(87)90021-5.
88. Sebé -Pedrós, A., Saudemont, B., Spitz, O., Tanay, A., and Marlow, H. (2018). Cnidarian Cell Type Diversity and Regulation Revealed by Whole-Organism Single-Cell RNA-Seq. Cell *173*, 1520–1534.e20. https://doi.org/10.1016/j.cell.2018.05.019.
89. Zimmermann, B., Montenegro, J.D., Robb, S.M.C., Fropf, W.J., Weilguny, L., He, S., Chen, S., Lovegrove-Walsh, J., Hill, E.M., Chen, C.-Y., et al. (2023). Topological structures and syntenic conservation in sea anemone genomes. Nat. Commun. *14:1-16*. https://doi.org/10.11038/s41467-023-44080-7.
90. Gasteiger, E., Hoogland, C., Gattiker, A., Duvaud, S., Wilkins, M.R., Appel, R.D., and Bairoch, A. (2005). Protein Identification and Analysis Tools on the ExPASy Server. In The Proteomics Protocols Handbook Springer Protocols Handbooks, J.M. Walker, ed. (Humana Press), pp. 571–607. https://doi.org/10.1385/1-59259-890-0:571.

## STAR★METHODS

### KEY RESOURCES TABLE

| REAGENT or RESOURCE | SOURCE | IDENTIFIER |
|---|---|---|
| Oligonucleotides | | |
| Primers for transgenes, see Table S2 | This study | N/A |
| Primers for promoter sequences, see Table S3 | This study | N/A |
| Recombinant DNA | | |
| SpCARP1 | IDT DNA | NCBI: KC148537 |
| SpSM30 | IDT DNA | NCBI: NP_999766.1 |
| MmAMBN | Genscript | NCBI: NM_001303431.1 |
| pCS2+8CmCherry | Addgene | RRID:Addgene_34935 |
| pNvT-MHC:mCherry | Addgene | RRID:Addgene_67943 |
| pKHR4 | Addgene | RRID:Addgene_74592 |
| Other | | |
| AscI | NEB | #R0558 |
| ClaI | NEB | #R0197 |
| PacI | NEB | #R0547 |
| SpeI | NEB | #R3133 |
| NotI | NEB | #R0189 |
| I-SceI | NEB | #R0694 |
| mMessage mMachine SP6 Transcription Kit | Invitrogen | AM1340 |
| MEGAclear Transcription Clean-Up Kit | Invitrogen | AM1908 |
| GeneJET Miniprep Kit | ThermoFisher | Cat# K0503 |
| Calcein Blue | Sigma | M1255 |
| CellMask | Fisher Scientific | C37608 |

### RESOURCE AVAILABILITY

#### Lead contact

Further information and requests for resources and reagents will be fulfilled by the lead contact, Mark Q. Martindale (mqmartin@whitney.ufl.edu).

#### Materials availability

Animals, reagents, and plasmids generated in this study are available by request from the lead contact.

#### Data and code availability

- All data reported in this paper will be shared by the lead contact upon request.
- This paper does not report original code.
- Any additional information required to reanalyze the data reported in this paper is available from the lead contact upon request.

### METHOD DETAILS

#### Animal culture

Adult *Nematostella vectensis* were maintained in 1/3X filtered seawater (FSW) diluted in deionized water and spawned following protocols as described previously.[60,74,75]

#### Molecular cloning and in vitro mRNA transcription

As a proof-of-principle, we focused on a Coral Acid-Rich Protein (CARP) from a stony coral (*Stylophora pistillata*). SpCARP1 is a membrane-associated IDP that binds $Ca^{2+}$ ions to induce $CaCO_3$ precipitation and is believed to initiate biomineralization in *S. pistillata*.[29] To highlight the potential and versatility of our system for studying other forms of biomineralization, we also developed transgenic constructs for

expressing proteins involved in the formation of sea urchin spicules (*Strongylocentrotus purpuratus*: SpSM30) and mice teeth (*Mus musculus:* Ameloblastin, MmAMBN).

SpCARP1 (NCBI: KC148537) cDNA was synthesized by IDTDNA Inc. (idtdna.com). SpSM30 (NCBI: NP_999766.1) cDNA was first codon optimized using Codon Optimization OnLine (COOL)[76] and synthesized by IDTDNA Inc. (idtdna.com). MmAMBN cDNA (NCBI: NM_001303431.1) was ordered from Genscript (New Jersey, USA; clone ID: OMu67099). Primers for SpSM30 and MmAMBN (Table S2) were designed with Primer3.[77] All cDNA was cloned in frame into the pCS2+8CmCherry vector (RRID:Addgene_34935) using AscI (NEB #R0558) and ClaI (NEB #R0197) cut sites. The SpCARP1 insert was synthesized as a gene fragment by Twistbioscience (Twistbioscience.com) and consisted of flanking restriction sites, a Kozak sequence optimized for invertebrates (AAAAAA),[78] putative signal sequences native to *N. vectensis* (Calumenin: v1g117044 or Laminin A: v1g248148) replacing the predicted signal sequence in the SpCARP1 cDNA. A linker sequence (GGATCCGCTGGCTCCGCTGCTGGTTCTGGCGAATTC)[79] and TEV protease recognition site were included in SpCARP1 and SpSM30 inserts. *Nematostella* signal sequences were predicted using SignalP.[80] mRNA was *in vitro* transcribed from linearized plasmids following the protocols for the Invitrogen mMessage mMachine SP6 Transcription Kit (Invitrogen AM1340) and purified using the MEGAclear Transcription Clean-Up Kit (Invitrogen AM1908). See also Table S2.

## Isolation of promoter DNA sequences

In order to express engineered proteins at distinct times and in specific cell types, we cloned putative promoter sequences upstream of the transcriptional start sites for *Nematostella Ubiquitin* (v1g217964) and *Mucin* (v1g203270) genes (see Table S3 for coordinates and primers used for cloning promoter sequences). Sequences were identified using the *Nematostella vectensis* genome 1.0[81] and amplified from gDNA extracted from whole embryos or adult tentacle clips using standard PCR procedures. To initially test for promoter activity, DNA fragments were cloned into the pNvT-MHCmCherry vector (RRID:Addgene_67943) using PacI (NEB #R0547) and AscI (NEB #R0558) sites, thereby replacing the myosin heavy chain (MHC) promoter. Confirmed plasmids were prepared following the protocol for the GeneJET Miniprep kit (ThermoFisher cat. #K0503). Sequences were confirmed via standard Sanger sequencing (Psomagen.com). When later cloned into pCS2+8-CmCherry vector (see next section), the promoter sequences were cut out using SpeI (NEB #R3133) and AscI (NEB #R0558) sites (see Figure S6).

## Generation of expression constructs for transgenesis

The software programs Serial Cloner V2.6 and Geneious Prime 2021.2.2 (https://www.geneious.com) were used to design transgenic constructs. The inserts were first cloned in frame into a pCS2+8CmCherry vector ( RRID:Addgene_34935) using AscI (NEB #R0558) and ClaI (NEB #R0197) sites. Promoter sequences were then inserted upstream using SpeI (NEB #R3133) and AscI (NEB #R0558) sites. Finally, fragments containing promoter and fusion protein segments were digested and cloned into the pKHR4 vector (RRID:Addgene_74592) using SpeI (NEB #R3133) and NotI (NEB #R0189) sites. The pKHR4 vector contains I-SceI (NEB #R0694) endonuclease recognition sites flanking the multiple cloning site that was replaced with our inserts.

## Microinjection

Fertilized eggs were prepared for microinjection as described previously.[60] Plasmids were incubated with 10X Cutsmart buffer and yeast I-SceI endonuclease (NEB #R0694) at 37°C for approximately 30 min prior to injection and then mixed with either Rodamine Green or Alexa 488 conjugated Dextran (0.2 mg/mL final concentration). Plasmids were injected in a final concentration of approximately 25 ng/μL. mRNA was diluted in nuclease-free water and mixed with nuclease-free Rodamine Green Dextran (0.2 mg/mL) and injected in final concentrations between 100 and 300 ng/μL.

## Fixation and confocal microscopy

Animals were either live-imaged or fixed 24 h postfertilization (hpf), 96 hpf, or 1-week post-injection as previously described.[82,83] Live animals were mounted in 1/3X FSW. Fixed animals were then washed in PBS-Tween, stained for DAPI and Alexa 488 Phalloidin, and mounted on glass slides in either 80% glycerol or PBS. All animals were imaged on a Zeiss Imager. Z2 or a Zeiss 710 laser scanning confocal microscope. Confocal images were Z-stacked with max intensity in FIJI[84] to show fluorescent signal.

## Water enrichment and calcein incubation

For both the non-enriched and enriched 1/3X FSW, temperature and pH (NBS scale) were measured using a pH/ATC electrode (Thermo Fisher Scientific, Waltham, USA), calibrated using pH 4, pH 7, and pH 10 buffer solutions (Thermo Fisher Scientific, Waltham, USA). Measurements of pH were conducted once on each solution used to incubate polyps for 1 h inside petri dishes. Salinity was measured using a digital refractometer (Milwaukee Instruments, Rocky Mount, USA). Measurements of total alkalinity (TA) were performed using an alkalinity test kit based on drop count titration (sulfuric acid) (Hach, Loveland, USA). Parameters of seawater carbonate system were calculated from pH, TA, temperature, and salinity using the CO2SYS package[85] with constants from Merbach et al.[86] as refit by Dickson and Millero[87] (see Table S4).

The concentration of calcium and carbonate ions regulate the thermodynamic driving force that determines the precipitation of calcium carbonate in biomineralizing animals.[53,71] To replicate biomineralization-favorable conditions, we incubated 1-month-old *N. vectensis* injected with transgenic SpCARP1 constructs in either 10mM $CaCl_2$, 10 mM $NaHCO_3$, or 10mM $CaCl_2$ + 10mM $NaHCO_3$ in 1/3X FSW for 1 h

in a cell culture Petri dish (5 mL). Polyps were then transferred to a new dish and incubated for another hour in a Calcein Blue solution (2.6 μM; Sigma 54375-42-2). Polyps were rinsed for 30 min in 1/3X FSW, then immobilized by adding 7.14% MgCl2 before imaging with a Zeiss 710 confocal microscope. Samples were observed with the mCherry red fluorescent filter (range 415–735nm) and the DAPI blue fluorescence filter (range 410–495nm) using 40× magnification. All imaging settings were kept constant between the samples. Images were acquired with the ZEN 2011 software (v14.0.0.0; Zeiss, United States) and processed in FIJI.[84]

### Fluorescence intensity

Mean mCherry fluorescence intensities per $\mu m^3$ of imaged individual were determined for a subset of planulae and primary polyps using the mean gray value in Fiji[84] and computing the volume using the Fiji plugin 'voxel counter.' Fluorescence intensity measurements were tested for normality (Shapiro-Wilk test) and homogeneity of variance (Levene's test). Statistical significance ($p < 0.05$) was assessed with parametric unpaired t-test (calcein and mCherry fluorescence in tentacles) and non-parametric Mann–Whitney test (mCherry fluorescence in entire planulae and polyps) using the GraphPad Prism software (v9.0.0) (GraphPad Inc., San Diego, CA, USA).

### Single cell dissociations

Injected embryos were dissociated 24 h post injection in 1/3X Ca2+/Mg2+-free and EDTA-free artificial seawater as previously described.[88] Dissociated cells were incubated for 1 h in 1:5000 CellMask (Fisher Scientific C37608), then washed two times in the dissociation media. Cells were water-immersed and imaged on a Zeiss Imager.Z2 at 40× magnification.

### Analysis of protein sequences and their amino acid composition

The partial protein sequences of NvCaluF used in Mass et al.[29] were retrieved from NCBI GenBank and Nematostella genome 1.0 (https://mycocosm.jgi.doe.gov/Nemve1/) while the full length protein sequence of NvCaluF (XP_001641982) encoded by NVE221 was found using the Nematostella genome 2.0 (https://simrbase.stowers.org/starletseaanemone)[89] and NCBI protein server (https://www.ncbi.nlm.nih.gov/Protein). Predictions of signal sequence in NvCaluF (XP_001641982) and SpCARP1 (NCBI: KC148537) were performed by SignalP 6.0 (https://services.healthtech.dtu.dk/services/SignalP-6.0/). Molecular weight, Theoretical pI and amino acids composition for NvCaluF and SpCARP1 protein sequences was calculated using ProtParam (https://web.expasy.org/protparam/).[90] SpCARP1 protein sequence from Mass et al.[29] was used for this comparison.